Published in final edited form as:
Magn Reson Med. 2010 August ; 64(2): 527–535. doi:10.1002/mrm.22449.

Absence of a Significant Extravascular Contribution to the Skeletal Muscle BOLD Effect at 3T

Otto A. Sanchez[1,2], **Elizabeth A. Copenhaver**[1,2], **Christopher P. Elder**[1,2], and **Bruce M. Damon**[1,2,3,4,5]

[1]Institute of Imaging Science, Vanderbilt University, Nashville TN, USA

[2]Department of Radiology and Radiological Sciences, Vanderbilt University, Nashville TN, USA

[3]Department of Biomedical Engineering, Vanderbilt University, Nashville TN, USA

[4]Department of Molecular Physiology and Biophysics, Vanderbilt University, Nashville TN, USA

[5]Program in Chemical and Physical Biology, Vanderbilt University, Nashville TN, USA

Abstract

Blood oxygenation-level dependent (BOLD) contrast in skeletal may reflect the contributions of both intravascular and extravascular relaxation effects. The purpose of this study was to determine the significance of the extravascular BOLD effect in skeletal muscle at 3T. In experiments, R_2* was measured before and during arterial occlusion under the following conditions: 1) the leg extended and rotated (to vary the capillary orientation with respect to B_0) and 2) with the blood's signal nulled using a multi-echo vascular space occupancy experiment. In the leg rotation protocol, 3 minutes of arterial occlusion decreased $\%HbO_2$ from 67% to 45% and increased R_2* from 34.2 to 36.6 s^{-1}, but there was no difference in the R_2* response to occlusion between the extended and rotated positions. Numerical simulations of intra- and extravascular BOLD effects corresponding to these conditions predicted that the intravascular BOLD contribution to the R_2* change was always >50 times larger than the extravascular BOLD contribution. Blood signal nulling eliminated the change in R_2* caused by arterial occlusion. These data indicate that under these experimental conditions, the contribution of the extravascular BOLD effect to skeletal muscle R_2* was too small to be practically important.

Keywords

mfMRI; extravascular BOLD effect; oxygenation; vessel orientation; VASO

INTRODUCTION

Variations in the rates of permanent and effective transverse relaxation (R_2 and R_2*, respectively) or in T_2-weighted signal may be used to evaluate the hemodynamic, metabolic and structural changes associated with muscle contractions (1), an approach known as muscle functional MRI (mfMRI) (2). During and following muscle contractions, changes in muscle R_2 and R_2* result from increases in intracellular water content, secondary to metabolite accumulation (3,4); variations in intracellular pH (4-6); and changes in the concentrations of paramagnetic molecules such as deoxyhemoglobin, as reflected in the blood oxygenation level dependent (BOLD) effect (7,8). The magnitude of each of these

Address for correspondence: Bruce M. Damon, 1161 21st Ave S, MCN-AA1105, Nashville TN USA 37232-2310, bruce.damon@vanderbilt.edu, Web: http://vuiis.vanderbilt.edu, Phone: (615) 322 8355, FAX: (615) 322 0734.

changes, and thus the variations in R_2 and R_2*, depend on the exercise and intensity (9), the muscle fiber type composition (3), and whole-body aerobic capacity (10). Since these factors affect R_2 and R_2* to different degrees, quantifying the independent contributions of and interactions among these factors is important to interpret physiological and pathological variations in muscle R_2 and R_2*.

Regarding the source of oxygen-level dependent contrast in skeletal muscle, it is noteworthy that skeletal muscle cells themselves contain several potential magnetic field perturbers that may also contribute to susceptibility-related signal decay in skeletal muscle. However, both theoretical calculations and experimental observations suggest that a true BOLD effect, and not a muscle oxygenation level dependent effect, occurs in skeletal muscle (8). The presence of a muscle BOLD effect has allowed the development of several new protocols for studying skeletal muscle physiology and pathophysiology. For example, Meyer *et al.* (11), with subsequent modifications by Damon *et al.* (12), have proposed the use of BOLD and proton-density weighted signals to studying microvascular and metabolic recovery following brief isometric contractions. In addition, several studies have proposed BOLD imaging protocols based on the Fick principal; in these protocols, constant muscle oxygen consumption with perfusion increases brought about by vasodilator infusion increase BOLD-dependent signal (13).

Because of the potential for using such protocols to assess muscle function, it is important to understand the biophysical basis of BOLD contrast in skeletal muscle, including the relative contributions of intravascular and extravascular relaxation effects. The intravascular BOLD effect refers to the effect of oxyhemoglobin saturation (%HbO_2) and the hematocrit on the relaxation of blood water (14,15). Intravascular BOLD phenomena result from the effects of chemical exchange between free intracellular water and water in the hydration shell of deoxyhemoglobin and/or diffusion through the magnetic field gradient surrounding deoxyhemoglobin (14,16-18); because the transmembrane exchange of water is rapid on the T_2 timescale (18), the relaxation of the blood as a whole is affected. The extravascular BOLD effect describes the effect of magnetic susceptibility gradients surrounding blood vessels on the relaxation of extravascular spins; in addition to %HbO_2 and hematocrit, this effect depends also on blood volume, the diffusion coefficient of water perpendicular to the vessels ($D\perp$), vessel radius, and the orientation of blood vessels with respect to B_0 (α) (19,20). In skeletal muscle at resting length, 90% of the length of capillaries is parallel to skeletal muscle fibers (21,22). Because many muscles have oblique fiber orientations and these orientations change during contraction (23), the predominant orientation of the blood vessels will also vary. If the extravascular BOLD effect is a significant contributor to R_2* in skeletal muscle, these factors would confound the simple interpretation of BOLD phenomena as reflecting physiological factors only by introducing a structural dependence to the BOLD effect.

Although previous numerical simulations (11,13,24) have predicted that extravascular BOLD effects in skeletal muscle are small, we know of no experimental studies that have evaluated extravascular BOLD effects and their contribution to skeletal muscle R_2*. Therefore, the purpose of this study was to use empirical evidence to test for extravascular BOLD contribution to skeletal muscle R_2* at 3.0T. In the first experiment, we tested the hypothesis that if there is a practically significant extravascular BOLD effect in skeletal muscle at 3.0 T, then the $\sin^2(\alpha)$ dependence of the chemical shift difference between the blood and tissue parenchyma (19,20) would cause R_2* to increase with α and also cause the effect of %HbO_2 changes on R_2* to increase with α. In addition, we evaluated the extravascular BOLD effect by determining the change in R_2* before and during ischemia while nulling the MR signal from inflowing blood using an inversion recovery sequence configured according to the vascular space occupancy (VASO) scheme (25). Following an

inversion pulse, because of the different T_1 values of the blood (1624 ms) (26) and the muscle tissue (1420 ms) (27), the times at which the magnetization originating in the blood and the magnetization from the muscle tissue cross the zero line differ. To test for an extravascular BOLD effect, we acquired images at the time corresponding to blood signal nulling. Under this circumstance any changes in R_2* reflect the contribution from extravascular BOLD effect. We expected that R_2* would not differ between the non-occlusion and occlusion conditions when the signal from the inflowing blood is eliminated. Finally, we used numerical models to aid in interpreting the observed experimental effects and to understand the external validity limits of our experimental findings.

MATERIALS AND METHODS

Subjects

This study was approved by the Vanderbilt University Institutional Review Board and was in accordance with the principals of the Declaration of Helsinki. Ten male volunteers free of known acute or chronic medical conditions and having age=23.7 ± 3.5 years (mean ± standard deviation), body mass index=23.6 ± 2.1 and ankle brachial index (ABI) =1.03 ± 0.08, reflecting healthy peripheral vasculature (28) were informed of the potential risks and benefits of the study and provided written informed consent to participate.

Study Procedures

Participants reported to the lab for an orientation and a testing session. During the orientation session, subjects completed an MRI screening form and a health history questionnaire. To calculate the ABI, blood pressure was measured at the brachial and dorsal pedis arteries. For the testing session, the subjects were asked not to consume any alcohol and to avoid moderate or heavy exercise for 24 hours prior to the testing session. Additionally, subjects were asked not to drink caffeinated beverages or smoke tobacco during the six hours prior the test. To test the significance of the extravascular BOLD effect, two protocols were used (Table 1). For the first protocol (leg rotation protocol), the potential effect of α on R_2* was determined by changing the orientation of the leg with respect to B_0 under occlusion and non-occlusion conditions. For the second protocol (blood signal nulling protocol) R_2* was measured before and during cuff occlusion when the signal from the blood was eliminated using VASO.

Five subjects participated in the leg rotation protocol. Each participant lay supine in the MRI scanner and a series of images of the leg was acquired while the leg was fully extended or partially flexed at a knee angle of about 40°, as measured using a goniometer. The subjects were instructed to lie passively (*i.e.*, not contract the muscles) during the procedure. In each leg orientation, the foot angle was 90 ° to avoid T_2 changes related to sarcomere overlap (29). In each position, the subjects were studied with and without proximal arterial occlusion. Arterial occlusion was accomplished by placing a blood pressure cuff at the mid-thigh and rapidly (<1 s) inflating it to 240 mm/Hg using a rapid cuff inflator (Hokanson Model E20, Bellevue, WA) for a total occlusion duration of 3 minutes. Five other participants completed the blood signal nulling protocol. A series of images was acquired 30 s before, during 3 minutes, and for 45 s following the cuff occlusion procedure. The leg was in the extended position and the foot was held at 90°. The cuff occlusion procedure was performed as for the leg rotation protocol.

Near Infrared Spectroscopy (NIRS) Data Acquisition

NIRS-measured $\%HbO_2$ and total hemoglobin concentration ([THb]) were determined for both experiments. $\%HbO_2$ and [THb] were measured concurrently to the MRI acquisition using a frequency domain, multi-distance NIRS oximeter using an MRI compatible emitter-

detector probe (Model 96208; ISS Inc. Champaign, IL). The operation of the system has been described in detail previously (30). Briefly, the system was calibrated before initiating the experimental procedures. The border of the tibialis anterior (TA) muscle was located by requesting the participant to dorsiflex. The NIRS probe was placed on the skin over the muscle and slightly distal to the surface coils. The NIRS probe was held in place by an elastic strap and was covered with a dark cloth to prevent interference from visible light. The strap was tightened only enough to avoid probe motion and to cause as little discomfort and anatomic distortion as possible. [THb] and $\%HbO_2$ were calculated according to the manufacturer's algorithms. The mean values during the initial 20 s before cuff occlusion and the last 20 s of the cuff occlusion were used in subsequent analyses.

MRI Data Acquisition

MRI data were obtained on a 3T Philips Intera/Achieva MR imager/spectrometer using a pair of 14×17 cm flexible surface coils placed over the anterior compartment of the right leg. After acquiring scout images in three planes, a volume of interest was specified in the leg and used for second-order shimming. A T_1-weighted anatomical image was obtained at the maximum girth of the leg with repetition time (TR)/echo time (TE)=500/16 ms, slice thickness (ST)=10 mm, one slice, field of view (FOV)=18×18 cm, matrix size=256×256, and number of excitations (N_{EX})=2. For the leg rotation protocol, R_2* was measured using a dual gradient-echo, dynamic EPI sequence with TR/TE=2000/6, 46 ms with ST=6 mm, acquired matrix=64×64 (reconstructed at 128×128), and the other geometric parameters of the anatomical image. Dynamic images were acquired for 30 s before, during, and for one minute following cuff occlusion in the extended and the rotated positions. As noted above, muscle fiber orientation was assumed to reflect α (21,22). To estimate the local muscle fiber orientation using the first eigenvector of the diffusion tensor (31,32), diffusion weighted images were acquired in fifteen diffusion directions using: TR/TE=4000/49 ms, diffusion weighting (b) value=500 sec/mm^2, N_{EX}=4, and the same geometric parameters as for the functional images. For the VASO protocol, R_2* was measured using a dynamic, non-slice selective GRE-EPI inversion recovery sequence with an inversion time (TI)=1125 ms and TR/TE=8500/10, 50 ms. This TI was based on the average T_1 values of arterial and venous blood, as noted above.

MRI Data Analysis

The Philips Research Imaging Development Environment (PRIDE) diffusion registration program, version 4.1 was used to register the diffusion-weighted images to the b=0 images with an affine transformation algorithm. Then, parametric maps of the tensor's eigenvalues (λ_1, λ_2 λ_3), first eigenvector (ε_1), and the ADC values were calculated using the PRIDE fiber tracking software version 4.1. Custom-written Matlab v. 7.5.0 (The Mathworks, Natick, MA, USA) routines were used to define a region of interest (ROI) around the TA muscle, carefully excluding resolved vessels and connective tissues. The TA muscle was chosen because the distribution of muscle fiber orientations with respect to B_0 is spatially uniform in each compartment of this muscle (33). Within the ROI, the mean orientation of ε_1 with respect to B_0 was calculated as the arccosine of the inner product of ε_1 and a unit vector in the Z direction. The mean values for ADC, λ_1, λ_2, λ_3 and R_2* were also calculated in the ROI; λ_3 was used to represent D⊥. For R_2* calculations from either protocol, the mean signal (S) in the ROI was measured for 30 seconds before and during the final 30 seconds of cuff occlusion. R_2* was calculated as:

$$R_2^* = \frac{\mathrm{In}\left(S_1 / S_2\right)}{\Delta TE} \quad [1]$$

where the subscripts 1 and 2 indicate the first and second echoes, respectively.

Statistical Analysis of Experimental Data

Data are presented as mean ± SE. For the leg rotation protocol, a general linear model repeated measured analysis was performed to test for main effects of position and occlusion and the position×occlusion interaction. A non-significant position main effect and a non-significant position×occlusion interaction would indicate that the effect of $\%HbO_2$ on R_2* does not depend on the leg position, providing evidence against an extravascular BOLD effect. For the blood nulled protocol, a paired Student's *t*-test was performed to test for differences in variables before and at the end of cuff occlusion. Statistical significance was set at $p<0.05$.

Numerical Simulations

Numerical simulations of the extravascular and intravascular BOLD effects were performed in Matlab v. 7.5.0. Extravascular BOLD simulations were performed essentially as previously described (24). Briefly, we calculated the magnetic susceptibilities for blood and tissue parenchyma by adapting procedures from Spees *et al*. (15). The mean chemical shift difference between the blood and tissue parenchyma was calculated using the infinite parallel cylinders model of Stables *et al.* (20). The gradient echo signal and R_2* were calculated for TE=30 ms using Eqs. 6 and 24 of Stables *et al.*, respectively. In the first set of simulations, we predicted the extravascular and intravascular BOLD contributions to the R_2* difference between the free flow/straight leg and the occluded flow/rotated leg conditions of the leg rotation protocol. We used the measured values of D⊥ and α and assumed blood volume percentages of 3.0 and 2.7% for free-flow and occlusion, respectively. Intravascular BOLD effects were simulated using the T_2* dependence of blood on $\%HbO_2$ at 3.0T reported in Ref. (34), interpolated for a hematocrit of 0.3.

We will use the experimental data and the first set of simulations to argue that the observed R_2* changes were due essentially entirely to intravascular BOLD phenomena. If so, then the difference between the mean R_2* values for the straight leg/occluded flow conditions measured by VASO and traditional gradient-echo acquisitions represents the blood's contribution to R_2* during occlusion. Further, the upper limit of its 95% confidence interval (95% CI) represents the magnitude of extravascular BOLD effects needed to increase the total BOLD effect significantly. In the second set of simulations we determined the values for D⊥, α, and the blood volume fraction that would have been necessary to have resulted in a significant extravascular BOLD effect. D⊥, α, and the blood volume fraction were varied because they change during and after exercise (23,35). Because different subjects participated in the two experiments, the 95% CI was formed using error propagation methods.

RESULTS

Experimental Protocols

Leg rotation protocol—Figure 1 shows the changes in the NIRS-observed data for the leg rotation protocol. $\%HbO_2$ did not differ between the extended and the flexed positions ($p=0.58$; Figure 1A), but decreased during occlusion (67.5 ± 2.7 vs. 45.5 ± 4.8 %; $p=0.002$; Figure 1A). There was not a significant position×occlusion interaction ($p=0.22$), indicating that the mean $\%HbO_2$ response to occlusion was similar in each leg position. [THb] did not differ between the extended and the rotated positions ($p=0.82$; Figure 2B) or when the cuff was inflated ($p=0.09$; Figure 2B). There was not a significant position×occlusion interaction ($p = 0.78$). Figures 2A and B show the changes in α and the diffusion tensor eigenvalues, respectively, due to leg rotation. The α increased when the leg was rotated from the

extended to the flexed position (from 17.1 ± 1.1 to 25.0 ± 3.0 °; p=0.047; Figure 2A). There were no differences in λ_1, λ_2, or λ_3 between the extended and the rotated conditions (p=0.56; Figure 2B). Figure 3A shows the changes in R_2* during the leg rotation protocol. R_2* increased during cuff occlusion from 34.2 ± 1.1 to 36.6 ± 1.4 s^{-1} (p=0.02), but did not differ between positions (p=0.35) and there was not a significant position×occlusion interaction (p=0.28).

Blood signal nulling protocol—During cuff occlusion, $\%HbO_2$ decreased from 59.7 ± 4.8 to 38.7 ± 3.4 % (p=0.002); [THb] decreased from 83.0 ± 5.2 to 76.5 ± 6.8 μM (p=0.02). There was no difference in the mean R_2* values before and at the end of cuff occlusion (33.7 ± 0.31 vs. 34.5 ± 0.6 s^{-1}; p=0.27) (Figure 3B).

Numerical Simulations

Figure 4A shows the predictions of the first set of simulations. The red solid line shows the extravascular BOLD contribution to R_2* for α =17.1°, $D\perp=1.31\times10^{-9}$ m^2/s, and 3% blood volume, corresponding to the free-flow/straight-leg condition. The blue solid line shows the extravascular BOLD contribution to R_2* for α =25.0°, $D\perp=1.28\times10^{-9}$ m^2/s, and 2.7% blood volume, that is, the occluded flow/rotated leg condition. Points on each curve are circled at the observed $\%HbO_2$ levels. The difference between the ordinates of these two points gives the extravascular BOLD contribution to the R_2* difference between these conditions (0.0245 s^{-1}). Also shown in each plot are the corresponding intravascular BOLD effects on the whole-tissue R_2* for blood volumes of 3.0% (red dashed line) and 2.7% (blue dashed line). The circled data points on these curves indicate the intravascular BOLD contribution to R_2* in the free-flow and occluded conditions; the R_2* difference between their ordinates is 0.79 s^{-1}. This value is similar to the experimentally observed effect (0.62 s^{-1}; Figure 3A) and more than an order of magnitude larger than the extravascular contribution. In Figure 4B, we present the ratio of modeled intravascular to extravascular BOLD effects for free flow/straight leg and occluded flow/rotated leg conditions. The circled points correspond to the observed $\%HbO_2$ levels. The ratios of intravascular to extravascular BOLD contributions to R_2* for the free flow/straight leg and occluded flow/rotated leg conditions were 558 and 61, respectively. The lowest modeled ratio was for the rotated leg with $\%HbO_2$=0%; the value was 36.

Figure 5 shows the results of the second set of simulations. The plain black line in panel A shows a weak dependence of the extravascular BOLD effect on D⊥ when blood volume=3%, α =17.1°, and $\%HbO_2$=40%; the dotted line shows the data for $\%HbO_2$=70%. The difference between the R_2* values observed during the flow-occluded periods of the conventional and VASO gradient echo experiments and its 95% CI was 3.08 s^{-1} ± 2.08 s^{-1}, with the value 2.08 s^{-1} shown as the horizontal gray line and representing the additional R_2* change needed to produce a significant extravascular BOLD effect. The data in Figure 5A indicate that there is no reasonable value of D⊥ that could raise the extravascular contribution to total BOLD effects to a significant level. Panel B shows the extravascular BOLD contribution to R_2* at α =0-90°. For blood volume =2%, 3%, and 4% and at $\%HbO_2$=40% (plain lines), a significant extravascular BOLD effect would begin to occur at α =52°, 46°, and 41°, respectively. The dotted lines, showing the data for $\%HbO_2$=70%, indicate that there is no reasonable blood volume fraction/α combination for which the extravascular BOLD contribution would be significant. Figure 5C shows that extravascular BOLD effect increases linearly with blood volume fraction, but at physiologically relevant levels is always less than the minimum threshold for a significant extravascular BOLD contribution; this is true both for $\%HbO_2$=40% and 70%.

DISCUSSION

The results of this study confirm and extend prior observations of a BOLD effect in skeletal muscle and provide evidence that under the experimental conditions employed, the extravascular BOLD effect in skeletal muscle is too small to be of practical significance. This conclusion is different from those concerning the role of the extravascular BOLD effect in the brain, but is supported by three lines of evidence: 1) the first set of simulations that predict a much smaller extravascular than intravascular BOLD effect for the experimental conditions employed; 2) the quantitative similarity of the BOLD effect across a physiologically significant range of capillary orientations; and 3) the absence of a significant BOLD effect under conditions of blood signal nulling. Within the limits defined by the second set of simulations, the absence of a practically significant extravascular BOLD effect in muscle at 3.0T means that muscle BOLD data from field strengths of 3.0T and below can be interpreted with intravascular mechanisms only.

Numerical Simulations Predict a Small Extravascular BOLD Effect

The simulations described in Figure 4 predict that for all $\%HbO_2$ levels and the levels of $D\perp$ and α encountered in the experimental studies, the extravascular BOLD effect is insignificant in comparison to intravascular BOLD effects. This finding is similar to those from models implemented by previous researchers, who have found that in skeletal muscle the extravascular BOLD effect is of very small magnitude. Meyer *et al.* (11) calculated that at 3.0T the extravascular BOLD effect following a 13% increase in $\%HbO_2$ would increase the BOLD-dependent signal by 0.5% compared to a 2.26% increase from the intravascular BOLD effect. Similarly, Utz *et al.* (13) estimated that the extravascular BOLD effect at 1.5T contributed to only 1% of the total BOLD signal.

One difficulty in modeling the extravascular BOLD effect is the need to account properly for the blood vessel geometry. One issue pertains to the distributions of vessel diameters and orientations in skeletal muscles. Branching in the arteriolar tree through five orders results in arterioles measuring between ~50 to 10 μm in diameter, which continue on to form capillaries and venules. However, because the capillaries constitute most of the vessels in the muscle tissue bed and 90% of their length is parallel to the muscle fibers (21,22), it is appropriate to model extravascular BOLD effects by treating capillaries as a collection of parallel, infinite cylinders. Another issue is how the vessel geometry affects the local magnetic field. We note that Frøhlich *et al.* (36) concluded that Stables *et al.*'s model underestimates the contribution of capillaries to susceptibility-induced relaxation rates by 55%, because of differing treatments of the capillary geometry. However, even increasing the contribution of the extravascular BOLD effect by twofold would still not have increased the relative importance of the extravascular BOLD effect to within an order of magnitude of the intravascular BOLD effect.

In summary, previously published and the present simulations predict a very small extravascular BOLD effect relative to the intravascular BOLD effect. These data provide the first line of evidence supporting the conclusion that the R_2* change due to arterial occlusion that we observed resulted almost entirely from intravascular BOLD phenomena.

No Effect of Leg Rotation on R_2*

In this protocol, we tested for an independent contribution of α on R_2* at different levels of $\%HbO_2$. We observed that R_2* increased by 2.4 s^{-1} at the end of cuff occlusion; for TE=46 ms, this would decrease T_2*-weighted signal by ~10%, similar in magnitude to the ~6% decrease in T_2*- weighted SI observed at the end of 5-7 minutes of cuff occlusion in previous reports (8,37). However, the magnitude of the R_2* effect did not differ when α was

changed (Figure 3A). Before interpreting this result, we first consider the influence of potential confounding variables.

As discussed above, transverse relaxation in skeletal muscle is influenced by many physiological factors. These include factors affecting a potential extravascular BOLD effect, the magnetic susceptibility effects of myoglobin, and metabolic contributions to R_2. Regarding influences on the extravascular BOLD effect, D⊥ and [THb] did not differ among the four experimental conditions (Figures 1B and 2B). In addition, capillary radii and hematocrit are not expected to change because of cuff occlusion or leg rotation. Therefore, the other contributors to extravascular BOLD effects were constant during the procedures. While in principle the paramagnetic effect of myoglobin may potentially affect the extravascular R_2*, Lebon *et al.* (8) showed a temporal incompatibility between the time courses of myoglobin desaturatation and the BOLD effect, indicating that the potential confounding effect of myoglobin may be eliminated as well. Concerning the metabolic influences on R_2, prolonged ischemia can increase lactate and inorganic phosphate (Pi) concentrations and decrease pH (38,39); these changes may decrease muscle R_2. However, Wilkie *et al.* (39) did not show any change in Pi or pH in the first 10 minutes of cuff occlusion and lactate only increased by 1 mmol/kg wet muscle weight. Therefore, it is very unlikely that those metabolic factors significantly altered the R_2* values during the short (3 min.) cuff occlusion procedure.

The remaining potential influences on the observed variations in R_2* are $\%HbO_2$ and α. Our implementation of the Stables *et al.* (20) model had predicted a very small extravascular BOLD contribution to R_2* (0.0245 s^{-1}) in comparison to the intravascular effect (0.79 s^{-1}). The lack of difference in the R_2* response to occlusion between the extended and rotated positions indicates that this small predicted extravascular contribution to R_2* is below the level of detection, adding a second line of evidence to support our conclusion that the R_2* change due to arterial occlusion in this study resulted almost entirely from intravascular BOLD phenomena.

No BOLD Effect when the Blood's Signal is Eliminated

In this protocol, we acquired multi-echo VASO data before and during arterial occlusion. By doing so, we eliminated the signal from the blood compartment and observed the resulting R_2* change due to arterial occlusion. If there were a significant extravascular BOLD effect, an R_2* increase would have occurred under these conditions. However, elimination the blood's signal also eliminated the BOLD effect, as reflected by the absence of a significant R_2* change (Figure 3B). The lack of change in R_2* under these experimental conditions adds a third line of evidence strongly supporting the argument that the extravascular BOLD effect was not a significant contributor to the observed R_2* changes in this study.

Conclusions and Implications

The results of the two experiments performed in this study and the first set of simulations, in concert with previously published simulated data (11,13), provide three independent lines of evidence to support the conclusion that the R_2* changes due to arterial occlusion observed experimentally resulted almost entirely from intravascular BOLD mechanisms. While the experimental studies used echo-planar imaging (EPI), which has a lower signal-to-noise ratio than conventional spin-warp acquisitions and therefore a reduced sensitivity for measuring small R_2* changes, we note that EPI has been used in a large number of dynamic imaging studies of skeletal muscle contractions (40-42). Therefore, the measurement conditions of the present study are highly relevant to how BOLD-dependent data in skeletal muscle are acquired.

This conclusion has practical implications for interpreting R_2* and R_2*-dependent signals in skeletal muscle. Specifically, it means that within the following limits to external validity, BOLD phenomena in skeletal muscle can be interpreted using intravascular mechanisms only. To define these limits, we start by noting that the statistical analysis of the experimental data necessarily treated the extravascular BOLD effect as a binary phenomenon (the result was either significance or non-significance). However, vessel geometry and other determinants of the extravascular BOLD effect are continuously distributed and at some point may cause the extravascular BOLD effect to become practically significant. Thus we used the second set of simulations (Figure 5) to determine the values, if any, for D⊥, α, and blood volume fraction at which the extravascular BOLD effect would become a significant contributor to total BOLD effects.

Figure 5A showed that for $\%HbO_2$ ranging from 40-70%, α=25°, and blood volume fraction =0.03, there was not a value of D⊥ that could result in a significant extravascular BOLD effect. The extravascular BOLD contribution to R_2* did vary weakly with D⊥, however. This weak dependence has two implications. First, it suggests that the static dephasing regime (SDR) does not exist around the capillaries of skeletal muscles, at least under the conditions assumed for the model. The product of the correlation time for water molecules to sample the magnetic environments near to and distant from the capillaries and the chemical shift difference between blood vessels and tissue parenchyma was always <0.11 for $\%HbO_2$=40% and <0.017 for $\%HbO_2$=70%. The values for this product are closer to meeting the criteria for the motional averaging regime, as defined by Kennan *et al.* (43), than for the SDR. The departure from the SDR probably results from the low values for δω that result from vessels closely oriented to B_0. These data also imply that any physiological alterations in D⊥ due to exercise probably do not alter the interpretation of R_2* data, as far as extravascular BOLD effects are concerned.

Unlike the case for D⊥, there can be values for α for which the extravascular BOLD effect may have statistical significance (Figure 5B). At $\%HbO_2$=40%, this transition begins in the range 41-56° (depending on the blood volume fraction). Therefore, the extravascular BOLD relaxation mechanism may need to be considered when examining BOLD effects during contractions in highly pennate muscles; to assess this possibility, α should be measured in relaxometry studies of such muscles. Figure 5C showed a strong, linear dependence of the extravascular BOLD effect on blood volume fraction. However, for any of the modeled values, the extravascular contribution never reached the level corresponding to statistical significance. Therefore, it is unlikely that changes in blood volume would require an interpretation of BOLD data that goes beyond intravascular mechanisms.

The final limits to generalization pertain to the static magnetic field strength. Because the chemical shift difference between blood and tissue that leads to the extravascular BOLD effect varies with field strength, the conclusion of the practical insignificance of the extravascular BOLD effect in skeletal muscle at 3.0T also applies to lower field strengths. However, at higher field strengths, extravascular BOLD phenomena may need to be considered.

Therefore, considering the experimental and model results from this study, those in the literature, and the just-discussed limitations to external validity, we conclude that at field strengths of 3.0T and below and for skeletal muscles with α<40° and $\%HbO_2$>40% or with α<25° and any value of $\%HbO_2$, the extravascular BOLD relaxation mechanism does not contribute significantly to total BOLD effects. This relaxation mechanism may need to be considered under other experimental conditions, however.

As a final point, we note the distinction between this conclusion from those regarding the role of this relaxation mechanism in the brain. In the brain, large relative contributions (up to 50% of total BOLD effects) have been predicted or observed experimentally (20,44,45). Figure 5C suggests that the difference between skeletal muscle and brain probably does not relate to the higher relative blood volume in the brain (5%). Rather, the difference between the extravascular BOLD effects in skeletal muscle and brain may be related to the distinct spatial distributions of capillaries between the two tissues. In the limb muscles, pennation angles are generally small and capillaries are oriented close to parallel to B_0; but in the brain, capillaries are spherically distributed (46). Accordingly, our model results predict that the contribution of the extravascular BOLD effect assuming parallel capillaries with $\alpha = 15°$ is >20 times smaller than the effect with the spherical distribution, for similar levels of blood volume and $\%HbO_2$.

Acknowledgments

This study was supported by grants from the National Institute of Arthritis and Musculoskeletal and Skin Diseases (NIH/NIAMS AR050101) and the National Center for Research Resources (NIH/NCRR M01 RR 00095 and UL1 RR024975). We thank Professors Malcolm J. Avison, Ph.D. and John C. Gore, Ph.D. for helpful discussions and Marti Chance for technical assistance.

References

1. Damon BM, Gore JC. Physiological basis of muscle functional MRI: predictions using a computer model. J Appl Physiol. 2005; 98(1):264–273. [PubMed: 15333610]
2. Meyer RA, Prior BM. Functional magnetic resonance imaging of muscle. Exerc Sport Sci Rev. 2000; 28(2):89–92. [PubMed: 10902092]
3. Prior BM, Ploutz-Snyder LL, Cooper TG, Meyer RA. Fiber type and metabolic dependence of T_2 increases in stimulated rat muscles. J Appl Physiol. 2001; 90(2):615–623. [PubMed: 11160061]
4. Damon BM, Gregory CD, Hall KL, Stark HJ, Gulani V, Dawson MJ. Intracellular acidification and volume increases explain R_2 decreases in exercising muscle. Magn Reson Med. 2002; 47(1):14–23. [PubMed: 11754438]
5. Fung BM, Puon PS. Nuclear magnetic resonance transverse relaxation in muscle water. Biophys J. 1981; 33(1):27–37. [PubMed: 7272437]
6. Louie EA, Gochberg DF, Does MD, Damon BM. Magnetization transfer and T_2 measurements of isolated muscle: effect of pH. Magn Reson Med. 2009; 61(3):560–569. [PubMed: 19097244]
7. Donahue KM, Van Kylen J, Guven S, El-Bershawi A, Luh WM, Bandettini PA, Cox RW, Hyde JS, Kissebah AH. Simultaneous gradient-echo/spin-echo EPI of graded ischemia in human skeletal muscle. J Magn Reson Imaging. 1998; 8(5):1106–1113. [PubMed: 9786149]
8. Lebon V, Brillault-Salvat C, Bloch G, Leroy-Willig A, Carlier PG. Evidence of muscle BOLD effect revealed by simultaneous interleaved gradient-echo NMRI and myoglobin NMRS during leg ischemia. Magn Reson Med. 1998; 40(4):551–558. [PubMed: 9771572]
9. Jenner G, Foley JM, Cooper TG, Potchen EJ, Meyer RA. Changes in magnetic resonance images of muscle depend on exercise intensity and duration, not work. J Appl Physiol. 1994; 76(5):2119–2124. [PubMed: 8063675]
10. Reid RW, Foley JM, Jayaraman RC, Prior BM, Meyer RA. Effect of aerobic capacity on the T_2 increase in exercised skeletal muscle. J Appl Physiol. 2001; 90(3):897–902. [PubMed: 11181598]
11. Meyer RA, Towse TF, Reid RW, Jayaraman RC, Wiseman RW, McCully KK. BOLD MRI mapping of transient hyperemia in skeletal muscle after single contractions. NMR Biomed. 2004; 17(6):392–398. [PubMed: 15468084]
12. Damon BM, Hornberger JL, Wadington MC, Lansdown DA, Kent-Braun JA. Dual gradient-echo MRI of post-contraction changes in skeletal muscle blood volume and oxygenation. Magn Reson Med. 2007; 47:670–679. [PubMed: 17390346]
13. Utz W, Jordan J, Niendorf T, Stoffels M, Luft FC, Dietz R, Friedrich MG. Blood oxygen level-dependent MRI of tissue oxygenation: relation to endothelium-dependent and endothelium-

independent blood flow changes. Arterioscler Thromb Vasc Biol. 2005; 25(7):1408–1413. [PubMed: 15890970]

14. Thulborn KR, Waterton JC, Matthews PM, Radda GK. Oxygenation dependence of the transverse relaxation time of water protons in whole blood at high field. Biochim Biophys Acta. 1982; 714(2):265–270. [PubMed: 6275909]
15. Spees WM, Yablonskiy DA, Oswood MC, Ackerman JJ. Water proton MR properties of human blood at 1.5 Tesla: magnetic susceptibility, T_1, T_2, T_2*, and non-Lorentzian signal behavior. Magn Reson Med. 2001; 45(4):533–542. [PubMed: 11283978]
16. Meyer ME, Yu O, Eclancher B, Grucker D, Chambron J. NMR relaxation rates and blood oxygenation level. Magn Reson Med. 1995; 34(2):234–241. [PubMed: 7476083]
17. Chen JJ, Pike GB. Human whole blood T_2 relaxometry at 3 Tesla. Magn Reson Med. 2009; 61(2): 249–254. [PubMed: 19165880]
18. Stefanovic B, Pike GB. Human whole-blood relaxometry at 1.5 T: Assessment of diffusion and exchange models. Magn Reson Med. 2004; 52(4):716–723. [PubMed: 15389952]
19. Yablonskiy DA, Haacke EM. Theory of NMR signal behavior in magnetically inhomogeneous tissues: the static dephasing regime. Magn Reson Med. 1994; 32(6):749–763. [PubMed: 7869897]
20. Stables LA, Kennan RP, Gore JC. Asymmetric spin-echo imaging of magnetically inhomogeneous systems: theory, experiment, and numerical studies. Magn Reson Med. 1998; 40(3):432–442. [PubMed: 9727947]
21. Kindig CA, Sexton WL, Fedde MR, Poole DC. Skeletal muscle microcirculatory structure and hemodynamics in diabetes. Respir Physiol. 1998; 111(2):163–175. [PubMed: 9574868]
22. Mathieu-Costello O. Capillary tortuosity and degree of contraction or extension of skeletal muscles. Microvasc Res. 1987; 33(1):98–117. [PubMed: 3550394]
23. Kawakami Y, Ichinose Y, Fukunaga T. Architectural and functional features of human triceps surae muscles during contraction. J Appl Physiol. 1998; 85(2):398–404. [PubMed: 9688711]
24. Damon B, Wadington M, Hornberger J, Lansdown D. Relative and absolute contributions of BOLD effects to the muscle functional MRI signal intensity time course: Effect of exercise intensity. Magn Reson Med. 2007 in press.
25. Lu H, Golay X, Pekar J, van Zijl P. Functional magnetic resonance imaging based on changes in vascular space occupancy. Magnetic Resonance in Medicine. 2003; 50(2):263–274. [PubMed: 12876702]
26. Lu H, Clingman V, Golay X, van Zijl P. Determining the longitudinal relaxation time (T_1) of blood at 3.0 Tesla. Magnetic Resonance in Medicine. 2004; 52(3):679–682. [PubMed: 15334591]
27. Gold GE, Han E, Stainsby J, Wright G, Brittain J, Beaulieu C. Musculoskeletal MRI at 3.0 T: relaxation times and image contrast. AJR Am J Roentgenol. 2004; 183(2):343–351. [PubMed: 15269023]
28. Hirsch AT, Haskal ZJ, Hertzer NR, Bakal CW, Creager MA, Halperin JL, Hiratzka LF, Murphy WR, Olin JW, Puschett JB, Rosenfield KA, Sacks D, Stanley JC, Taylor LM Jr, White CJ, White J, White RA, Antman EM, Smith SC Jr, Adams CD, Anderson JL, Faxon DP, Fuster V, Gibbons RJ, Hunt SA, Jacobs AK, Nishimura R, Ornato JP, Page RL, Riegel B. ACC/AHA Guidelines for the Management of Patients with Peripheral Arterial Disease (lower extremity, renal, mesenteric, and abdominal aortic): a collaborative report from the American Associations for Vascular Surgery/Society for Vascular Surgery, Society for Cardiovascular Angiography and Interventions, Society for Vascular Medicine and Biology, Society of Interventional Radiology, and the ACC/AHA Task Force on Practice Guidelines (writing committee to develop guidelines for the management of patients with peripheral arterial disease)--summary of recommendations. J Vasc Interv Radiol. 2006; 17(9):1383–1397. quiz 1398. [PubMed: 16990459]
29. Rump J, Braun J, Papazoglou S, Taupitz M, Sack I. Alterations of the proton-T_2 time in relaxed skeletal muscle induced by passive extremity flexions. J Magn Reson Imaging. 2006; 23(4):541–546. [PubMed: 16514596]
30. Maguire MA, Weaver TW, Damon BM. Delayed blood reoxygenation following maximum voluntary contraction. Med Sci Sports Exerc. 2007; 39:257–267. [PubMed: 17277589]

31. Cleveland GG, Chang DC, Hazlewood CF, Rorschach HE. Nuclear magnetic resonance measurement of skeletal muscle: anisotropy of the diffusion coefficient of the intracellular water. Biophys J. 1976; 16(9):1043–1053. [PubMed: 963204]
32. Damon BM, Ding Z, Anderson AW, Freyer AS, Gore JC. Validation of diffusion tensor MRI-based muscle fiber tracking. Magn Reson Med. 2002; 48(1):97–104. [PubMed: 12111936]
33. Lansdown DA, Ding Z, Wadington M, Hornberger JL, Damon BM. Quantitative diffusion tensor MRI-based fiber tracking of human skeletal muscle. J Appl Physiol. 2007; 103(2):673–681. [PubMed: 17446411]
34. Zhao J, Clingman C, Närväinen M, Kauppinen R, van Zijl P. Oxygenation and hematocrit dependence of transverse relaxation rates of blood at 3T. Magnetic Resonance in Medicine. 2007; 58(3):592–597. [PubMed: 17763354]
35. Morvan D, Leroy-Willig A. Simultaneous measurements of diffusion and transverse relaxation in exercising skeletal muscle. Magn Reson Imaging. 1995; 13(7):943–948. [PubMed: 8583872]
36. Frohlich AF, Ostergaard L, Kiselev VG. Theory of susceptibility-induced transverse relaxation in the capillary network in the diffusion narrowing regime. Magn Reson Med. 2005; 53(3):564–573. [PubMed: 15723392]
37. Toussaint JF, Kwong KK, Mkparu FO, Weisskoff RM, LaRaia PJ, Kantor HL. Perfusion changes in human skeletal muscle during reactive hyperemia measured by echo-planar imaging. Magn Reson Med. 1996; 35(1):62–69. [PubMed: 8771023]
38. Hajnal JV, Roberts I, Wilson J, Oatridge A, Saeed N, Cox IJ, Ala-Korpela M, Bydder GM, Young IR. Effect of profound ischaemia on human muscle: MRI, phosphorus MRS and near-infrared studies. NMR Biomed. 1996; 9(7):305–314. [PubMed: 9134541]
39. Wilkie DR, Dawson MJ, Edwards RH, Gordon RE, Shaw D. ^{31}P NMR studies of resting muscle in normal human subjects. Adv Exp Med Biol. 1984; 170:333–347. [PubMed: 6741702]
40. Damon BM, Hornberger JL, Wadington MC, Lansdown DA, Kent-Braun JA. Dual gradient-echo MRI of post-contraction changes in skeletal muscle blood volume and oxygenation. Magn Reson Med. 2007; 57(4):670–679. [PubMed: 17390346]
41. Damon BM, Wadington MC, Lansdown DA, Hornberger JL. Spatial heterogeneity in the muscle functional MRI signal intensity time course: effect of exercise intensity. Magn Reson Imaging. 2008; 26(8):1114–1121. [PubMed: 18508220]
42. Jenner G, Foley JM, Cooper TG, Potchen EJ, Meyer RA. Changes in magnetic resonance images of muscle depend on exercise intensity and duration, not work. J Appl Physiol. 1994; 76(5):2119–2124. [PubMed: 8063675]
43. Kennan RP, Zhong J, Gore JC. Intravascular susceptibility contrast mechanisms in tissues. Magn Reson Med. 1994; 31(1):9–21. [PubMed: 8121277]
44. Lu H, van Zijl PC. Experimental measurement of extravascular parenchymal BOLD effects and tissue oxygen extraction fractions using multi-echo VASO fMRI at 1.5 and 3.0 T. Magn Reson Med. 2005; 53(4):808–816. [PubMed: 15799063]
45. Boxerman JL, Hamberg LM, Rosen BR, Weisskoff RM. MR contrast due to intravascular magnetic susceptibility perturbations. Magn Reson Med. 1995; 34(4):555–566. [PubMed: 8524024]
46. Nonaka H, Akima M, Hatori T, Nagayama T, Zhang Z, Ihara F. Microvasculature of the human cerebral white matter: arteries of the deep white matter. Neuropathology. 2003; 23(2):111–118. [PubMed: 12777099]

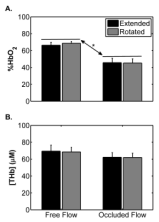

Figure 1.

Mean near infrared spectroscopy-measured %HbO_2 (A) and [THb] (B) levels by leg position with and without cuff occlusion for the leg rotation protocol. Error bars indicate the SE. The asterisk (*) indicates a difference between mean %HbO_2 levels between free flow and occluded flow conditions ($p = 0.002$); there was not a significant difference between positions ($p=0.58$) and the position×occlusion interaction was not significant ($p=0.22$). For [THb], there was not a significant difference between positions ($p = 0.82$) or due to occlusion ($p=0.09$) and the position × cuff occlusion interaction was not significant ($p = 0.82$).

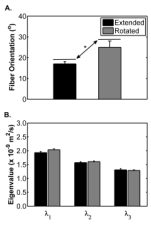

Figure 2.

Mean muscle fiber orientation with respect to B_0 (A) and first, second, and third eigenvalues of the diffusion tensor (B) by position during the leg rotation protocol. Error bars indicate the SE. The asterisk (*) indicates difference in fiber orientation between extended and rotated positions ($p = 0.047$). There were no significant differences between the mean values of the eigenvalues between the two positions.

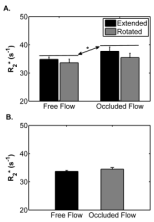

Figure 3.

Changes in mean R_2* leg in A) leg rotation protocol and B) blood signal nulling protocol. Error bars indicate the SE. In panel A, the asterisk (*) indicates a significant difference between the mean R_2* values for the free flow and occluded flow conditions; p = 0.02. There was neither a significant effect of leg position (p=0.35) nor a significant position×occlusion interaction (p=0.28), indicating that the R_2* response to occlusion was not affected by leg orientation. Panel B shows that eliminating the blood's signal caused the R_2* change due to flow occlusion not to be significant (p=0.27).

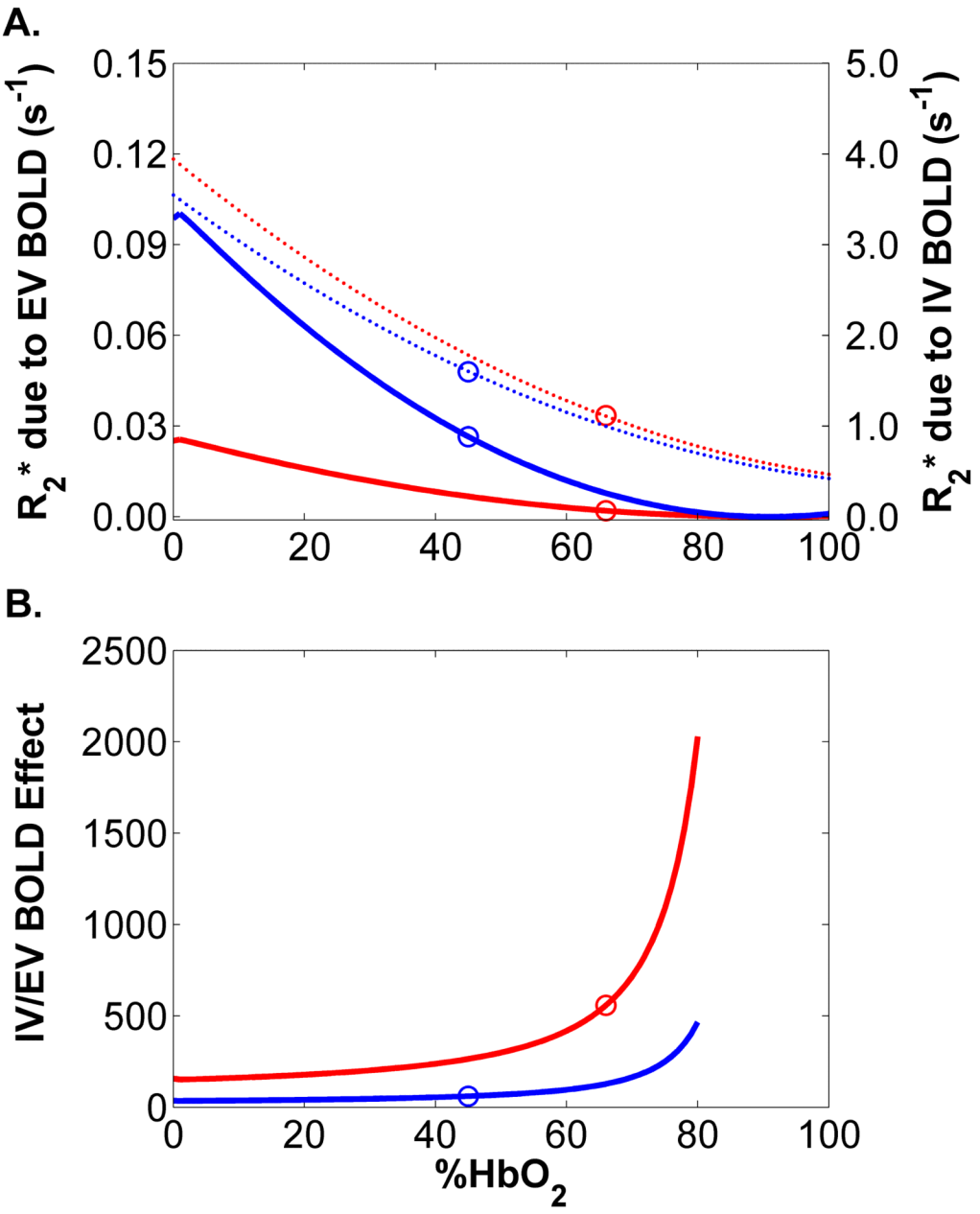

Figure 4.

Results from the first set of numerical simulations. A) Calculated intravascular and extravascular BOLD effects, for conditions designed to match the free flow/straight leg and occluded flow/rotated leg conditions of the leg rotation protocol. Solid lines depict the extravascular BOLD response and dashed lines depict the intravascular BOLD response; red lines show the free flow/straight leg condition and blue lines show the occluded flow/rotated leg condition. The circled points correspond to the measured %HbO_2 levels. The differences of ordinates of the points correspond to a 0.0245 s^{-1} extravascular R_2* effect and a 0.79 s^{-1} intravascular R_2* effect. B) Ratio of the intravascular-to-extravascular R_2* contributions, calculated using the data in Panel A. For all values of %HbO_2, the intravascular contribution is at least 100 times the extravascular contribution.

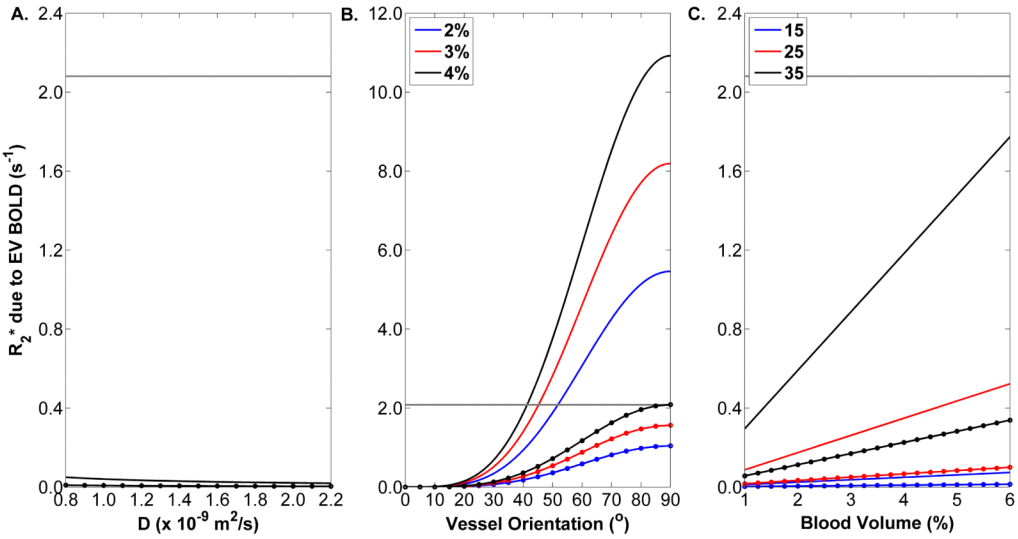

Figure 5.

Results from the second set of numerical simulations. A) The solid line indicates a weak dependence of the calculated extravascular BOLD effects on D⊥, for α =17.1°, 3% blood volume, and %HbO_2=40%; the dashed lines indicate the dependence for %HbO_2=70%. B) The solid lines indicate the dependences of the calculated extravascular BOLD effects on α for D⊥=1.31×10-9 m^2/s, three levels of blood volume (see legend), and %HbO_2=40%. The dashed lines indicate the dependences for %HbO_2=70%. Non-linear relationships, owing to the $sine^2(\alpha)$ dependence of the chemical shift difference between blood and tissue parenchyma, is seen. C) The solid lines indicate linear dependences of the calculated extravascular BOLD effects on relative blood volume for D⊥=1.31×10^{-9} m^2/s, three levels of α (see legend), and %HbO_2=40%. The dashed lines indicate the dependences for %HbO_2=70%.

Table 1

Experimental designs for the leg rotation and blood signal nulling protocols. R_2* was measured under each experimental condition indicated; note that the difference in R_2* between the free flow/straight leg conditions in the leg rotation and blood signal nulling protocols reflects the blood's contribution to R_2*. The diffusion tensor was measured only in the free flow conditions under the leg rotation protocol.

Protocol	Leg Position	Occlusion	
		No	Yes
Leg Rotation	Extended	Free flow/Straight leg	Occluded flow/Straight leg
	Rotated	Free flow/Rotated leg	Occluded flow/Rotated leg
Blood Signal Nulling	Extended	Free flow/Straight leg (VASO)	Occluded flow/Straight leg (VASO)